Proceedings of the ASME 2010 Conference on Smart Materials, Adaptive Structures and Intelligent Systems
SMASIS2010
September 28 - October 1, 2010, Philadelphia, Pennsylvania, USA

SMASIS2010-3843

VALIDATION AND CHARACTERIZATION OF AN ACOUSTIC SENSOR BASED ON PVDF MICROPILLARS AND PATTERNED ELECTRODES

Jian Xu
Smart Materials and Structures Laboratory
Smart Vehicle Concepts Center
Department of Mechanical Engineering
Ohio State University
Columbus, Ohio 43210
Email: xu.212@buckeyemail.osu.edu

Marcelo J. Dapino*
Smart Materials and Structures Laboratory
Smart Vehicle Concepts Center
Department of Mechanical Engineering
Ohio State University
Columbus, Ohio 43210
Email: dapino.1@osu.edu

Daniel Gallego-Perez
Ohio MicroMD Laboratory
Department of Biomedical Engineering
Ohio State University
Columbus, Ohio 43210
Email: gallego-perez.2@buckeyemail.osu.edu

Derek Hansford
Ohio MicroMD Laboratory
Department of Biomedical Engineering
Ohio State University
Columbus, Ohio 43210
Email: hansford.4@osu.edu

ABSTRACT

This paper addresses the fabrication, validation, and characterization of a millimeter-size acoustic sensor consisting of Polyvinylidene Fluoride (PVDF) micropillars and patterned electrodes. The sensor takes advantage of two key design principles: stress amplification through the area ratio between the overall surface exposed to acoustic waves and the area of the individual micropillars, and patterned electrodes which reduce the capacitance of the sensor by excluding the capacitance of the air between micropillars. In combination, these design principles enable a sensor capable of achieving 100$\times$ the sensitivity of flat PVDF film. A sensitivity analysis is presented and sensor fabrication details are described. An experimental setup was developed to characterize the sensor against a reference microphone. A signal conditioning circuit including a preamplifier circuit and a notch filter was designed and constructed. Sensitivity calibration tests show that a micropillar array with a gap ratio of 5.82 exhibits a stress constant $g_{33} = -19.93$ V/m/Pa, which is 60.39 times greater than the stress constant of commercial PVDF film. Experimental results also show that the sensitivity of the sensor is in close agreement with theory, thus confirming the performance advantages of the micropillar sensor.

Keywords: Microphone, PVDF sensor, micropillars, microfabrication

NOMENCLATURE

h pillar height
d pillar diameter
g_1 gap between pillars in x-direction
g_2 gap between pillars in y-direction
g_{33} piezo stress constant
ε_r relative permittivity of PVDF
$\bigtriangledown^2$ Laplacian operator

*Address all correspondence to this author.

ϕ velocity potential
c_0 speed of sound
f_c cut-off frequency of a circular tube
l tube length
τ time constant of a first-order system
ω_n natural frequency of a second-order system

INTRODUCTION

A variety of microphone designs are used in acoustic applications requiring a maximum sound pressure level (SPL) of 110-130 dB (re 20 μPa) and frequency bandwidth of 20 kHz or greater. Microphones for aeroacoustic measurements require even higher SPL in excess of 160 dB and frequency bandwidth on the order of 100 kHz, in part due to tightening regulatory constraints associated with airport noise standards. Such measurements are crucial for guiding and validating the development of accurate noise prediction tools and effective suppression techniques [1,2]. Therefore, there is a need for acoustic sensors capable of exhibiting extremely high sensitivity while simultaneously having a broader frequency range and wider dynamic range than the existing designs.

Another realization of microphones is electronic stethoscopes, which are commonly used for clinical auscultation and real-time monitoring of the human respiratory system. A significant volume of research is devoted to the analysis of lung sounds based on empirical information of normal and abnormal sounds [3, 4]. Electronic stethoscope arrays for measurement of breathing sounds are of great interest due to their non-invasive nature, yet the utilization of these arrays for real-time monitoring of lung sounds is confined to large sound fields in adults. The existing electronic stethoscopes are too bulky, typically 25 mm in diameter, for utilization in infants and small children.

The piezoelectric polymer Polyvinylidene Fluoride (PVDF), first discovered by Kawai [5], has been widely used in a wide range of military, industrial, and biomedical sensing applications [6–9]. PVDF can generate voltages 10-25 times higher than piezoceramics for the same pressure input. Perlman et al. [10] reported that the piezoelectric and pyroelectric constants of PVDF films and copolymers can be increased by nearly 200% when they are simultaneously subjected to stretching and poling. These polymers are quite stable because they can resist moisture, most chemicals, oxidants and intense ultraviolet and nuclear radiation. PVDF is synthesized by addition polymerization of the CH2=CF2 monomer, and exhibits α, β, γ and δ phases. The α phase is the lowest energy conformation and non-polar form. The γ and δ phases are not common. The β phase form, which has a net dipole moment pointing from the electronegative fluorine to the electropositive hydrogen, produces a net dipole moment nearly normal to the polymer chain [11]. Defect groups of head to head and tail to tail are believed to be responsible for the formation of β phase and hence for the piezoelectric properties of PVDF [12]. Non-porous PVDF films with very high β phase ratios were obtained via a very high pressure applied to porous PVDF films [13]. Sensors based on PVDF film are attractive due to their high sensitivity and low cost. For example, a PVDF film pressure sensor is used for in-sleep cardiorespiratory monitoring [14]. Uncooled infrared (IR) sensors using PVDF thin film are used to detect temperature changes from low levels of incident IR radiation [15].

Cochlea-inspired transducers investigated by Grosh et al. [16, 17] could achieve levels of miniaturization not possible with existing devices. A flexible tensioned membrane with an exponentially tapered width is employed to obtain a varying acoustic impedance, which can achieve cochlear-like frequency-position mapping. A rigid-walled duct filled with silicone oil is implemented to mimic the environment of the passive mammalian cochlea. Arnold et al. [18] designed a piezoresistive silicon microphone for aeroacoustic measurements that features a small size, high dynamic range, large frequency bandwidth, and low power consumption. The microphone consists of four dielectrically-isolated, single crystal silicon piezoresistors mounted on the top surface of a circular, tensile silicon nitride diaphragm. Several devices were investigated to characterize linearity, frequency response, drift, noise, and power. The sensors show a linear SPL up to 160 dB and a 52 dB noise floor, and consume 15 mW of power when operated at 3 V.

Horowitz at al. [19] developed a micromachined piezoelectric microphone for aeroacoustic measurements. The microphone was fabricated by combining a lead zirconate-titanate (PZT) deposition process on a silicon-on-insulator wafer with deep reactive ion-etching. An experimental setup in a plane-wave tube was used to characterize the microphone. The device exhibits a sensitivity of 0.75 μV/Pa, dynamic range of 47.8-169 dB and resonance frequency of 50.8 kHz. Wang et al. [20] built a PZT-based microacoustic sensor that employs interdigitated electrodes and in-plane polarization instead of commonly used parallel plate-electrodes and through-thickness polarization. The sensitivity is greatly improved because of the small capacitance of the interdigitated capacitor and the large and adjustable electrode spacing, as well as the advantage of the relatively larger piezoelectric stress constant g_{33}. Toda et al. [21] developed a contact vibration sensor made by bonding a piezoelectric PVDF film to a curved frame structure and a rubber piece with a front contact face. Pressure perpendicular to the PVDF film surface, transmitted from the rubber face, is converted to the internal circumferential stress that induces an electric charge due to the piezoelectric effect. An accelerometer mounted between the rubber face and a rigid vibration exciter plate was used to investigate the frequency response of the device, which shows the sensitivity has a flat range from 16 Hz to 3 kHz and a resonance peak at 6 kHz.

MEMS devices based on piezoelectric and ferroelectric materials have been applied in energy harvesting, electro-

mechanical sensing, microactuation, photonics, spintronics, and data storage [22–26]. Previous reports have studied the use of thin PVDF flat films in different MEMS applications [27–29]. Microstructured piezoelectric materials have the potential to provide improved performance and functionality to MEMS devices. Arrays of microfabricated PVDF pillars could provide enhanced sensitivity to acoustic signals compared to thin flat PVDF films [30].

The voltage produced by a capacitive sensor is given by the ratio between charge and capacitance. The acoustic sensor presented in this article exploits the key advantages of PVDF as a sensor material through two key design elements aimed at increasing the charge and decreasing the effective device capacitance. The first design element is a stress amplification mechanism through the area ratio between the overall surface exposed to acoustic waves and the area of the micropillars array (Figure 1(b)). Because PVDF responds to stress, the mechanical gain increases the amount of charge for a given pressure value. The second design element is top and bottom electrodes selectively patterned to form an overlapping active area determined by the micropillars. Excluding the capacitance of the other inactive area, the design with patterned electrodes reduces the capacitance of the sensor and hence increases the voltage it generates.

SENSITIVITY ANALYSIS

The static sensitivity is defined as the ratio of the output voltage over the pressure acting on the PVDF material,

$$K = V_o/P. \tag{1}$$

Figure 1 (a) shows the open circuit of a flat PVDF film sensor. The open circuit voltage generated across the film thickness is

$$V_o = -g_{33} \cdot \sigma \cdot h, \tag{2}$$

where g_{33} is the piezoelectric stress constant in the x_3-direction, σ is the stress induced in the material (in this case, $\sigma = P$), and h is the thickness of the PVDF film. Substitution of Eq. (2) into (1) gives the sensitivity as

$$K_1 = -g_{33} \cdot h. \tag{3}$$

We have proposed two sensor designs [30] which exhibit higher sensitivity than flat continuous film: PVDF micropillars with patterned electrodes, as shown in Figure 1(c), and with full electrodes, as shown in Figure 1(b) . The theoretical sensitivity of PVDF micropillars with patterned electrodes is

$$K_{mp} = \frac{(d+g_1)\cdot(d+g_2)}{\pi d^2/4} \cdot (-g_{33}) \cdot h. \tag{4}$$

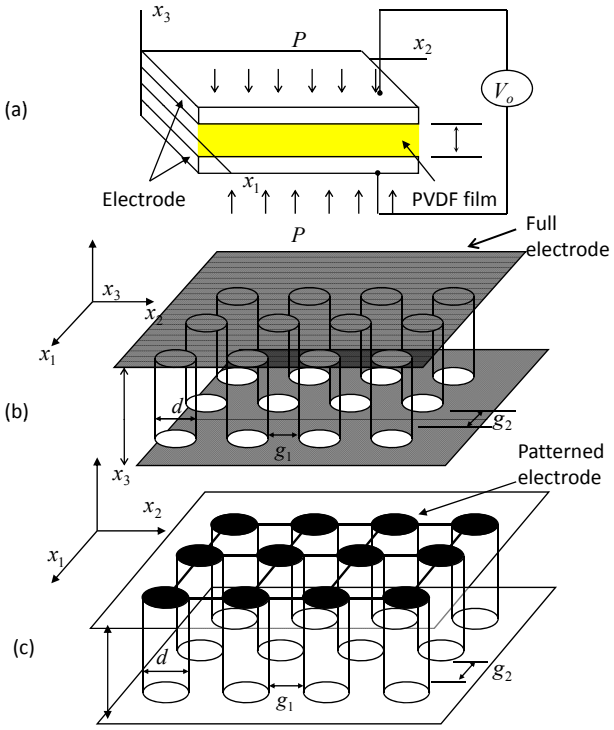

FIGURE 1. COMPARISON OF THREE DESIGNS. (A) SOLID PVDF FILM. (B) PILLAR PVDF WITH FULL ELECTRODES (C) PILLAR PVDF WITH PATTERNED ELECTRODES

The theoretical sensitivity of PVDF micropillars with full electrodes has the form [30]

$$K_{mf} = \frac{\varepsilon_r(d+g_1)(d+g_2)}{\pi d^2/4\cdot(\varepsilon_r-1)+(d+g_1)(d+g_2)} \cdot (-g_{33}) \cdot h. \tag{5}$$

Therefore, compared to the flat continuous PVDF film, the sensitivity amplification ratios of PVDF micropillars with patterned electrodes and with full electrodes are $(d+g_1)\cdot(d+g_2)/(\pi d^2/4)$ and $\varepsilon_r(d+g_1)(d+g_2)/[\pi d^2/4\cdot(\varepsilon_r-1)+(d+g_1)(d+g_2)]$, respectively. The respective stress constants are $(d+g_1)\cdot(d+g_2)/(\pi d^2/4)\cdot g_{33}$ and $\varepsilon_r(d+g_1)(d+g_2)/[\pi d^2/4\cdot(\varepsilon_r-1)+(d+g_1)(d+g_2)]\cdot g_{33}$. A comparison of the sensitivities of the two micropillar designs relative to that of solid PVDF film is shown in Figure 2. The micropillar sensor with patterned electrodes theoretically has an unlimited sensitivity with increasing geometry ratio g/d (assuming $g = g_1 = g_2$). A PVDF sensor based on micropillars and patterned electrodes with a gap ratio of $\sim$8 could achieve 100$\times$ the sensitivity of flat PVDF film. For the developed PVDF micropillar sensor with patterned electrodes, the gap ratio (g/d) of the sensor is 5.82.

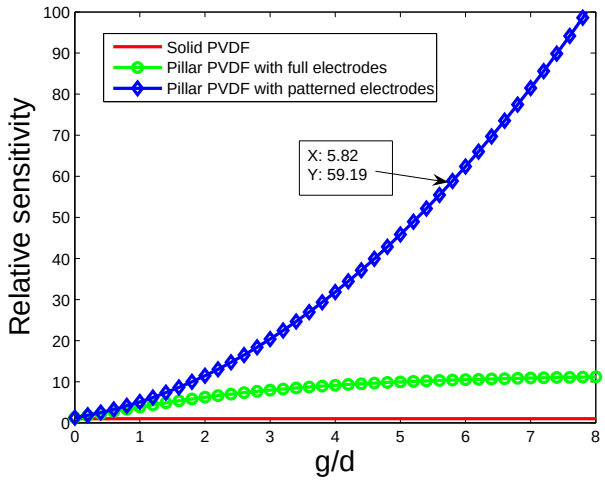

FIGURE 2. RELATIVE SENSITIVITY OF THE PROPOSED PVDF MICROPILLAR SENSOR WITH PATTERNED ELECTRODES COMPARED TO PVDF FILM AND FULLY ELECTRODED MICROPILLARS. THE GAPS ARE ASSUMED EQUAL ($g = g_1 = g_2$).

Therefore, the stress constant of the fabricated sensor is theoretically 59.19× larger than that of flat continuous PVDF film (Figure 2).

SENSOR FABRICATION

Patterned Electrode Fabrication

Figure 3 shows the photomask used for fabrication of the the patterned electrode. The mask contains six designs, and the one with the biggest gap ratio (left and bottom) was chosen for the fabricated sensor. The negative of the electrode pattern, which consisted of 11 μm diameter circles (∼64 μm spacing) interconnected by 2 μm wide lines, was first defined on a glass slide via photolithography using a positive photoresist (Shipley 1813). A ∼50 nm Au/Pd layer was then sputter-coated on the patterned surface, followed by acetone-assisted dissolution of the photoresist in a sonicator. The fabrication process and optical micrographs of the electrode are depicted in Figure 4.

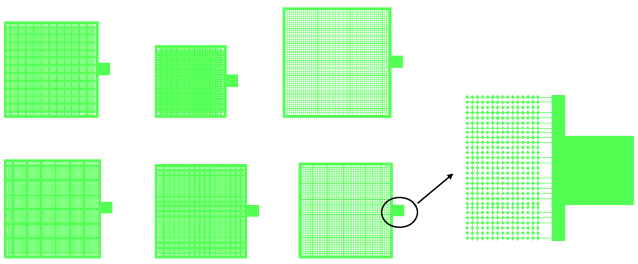

FIGURE 3. PHOTOMASK DESIGNED IN ADS.

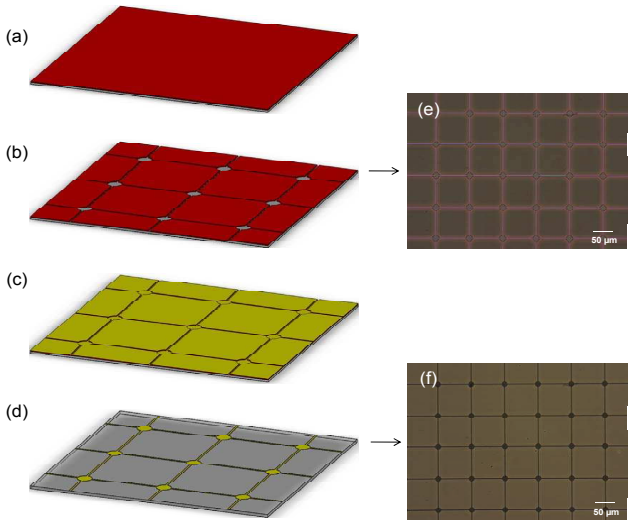

FIGURE 4. PATTERNED ELECTRODE FABRICATION. (A) PHOTORESIST IS DEPOSITED OVER THE GLASS SLIDE. (B) PHOTORESIST PATTERNING VIA PHOTOLITHOGRAPHY. (C) AU/PD LAYER IS DEPOSITED OVER THE PATTERNED SURFACE. (D) PHOTORESIST IS SELECTIVELY REMOVED WITH ACETONE. (E) AND (F) OPTICAL MICROGRAPHS OF THE PATTERNED PHOTORESIST AND PATTERNED ELECTRODE, RESPECTIVELY.

PVDF Microfabrication

PVDF micropatterning and poling was conducted via previously established techniques, described in more detail elsewhere [30,31]. Standard photolithography was used to define the footprint pattern of the sensor (11 μm diameter circles spaced by 64 μm) on a silicon master. A polydimethylsiloxane (PDMS) stamp bearing the negative replica of the pattern was created by pouring silastic T-2 PDMS (Dow Corning) mixed with its curing agent over the master, vacuum degassing and curing at room temperature for 48 hours before removal. Patterned PDMS stamps were then used for the fabrication of PVDF micropillars. Briefly, a 10 wt % PVDF (Aldrich) solution in dimethylacetamide (Sigma-Aldrich) and acetone was spin coated on the PDMS stamp at 1000 rpm for 45 seconds. The stamp was then heated up to ∼150^{o}C for 2-3 minutes to evaporate the solvent and anneal the PVDF. The micropatterned PVDF film was optically aligned with the patterned electrode, and bonded together via thermal pressing at ∼150^{o}C and 35 kPa for 5 minutes. Fig-

ure 5 illustrates the fabrication process of PVDF micropillars. Scanning electron microscopy (SEM) images of the patterned PVDF films are shown in Figure 5 (e) and (f). Cross sectional analysis via SEM confirmed that the patterned film had a thickness of 9.5 $\pm$0.18 μm (average $\pm$standard deviation). Finally, the PVDF pillars were overlaid with adhesive copper tape (3M), and poled by applying an electric field of $\sim$120 MV/m.

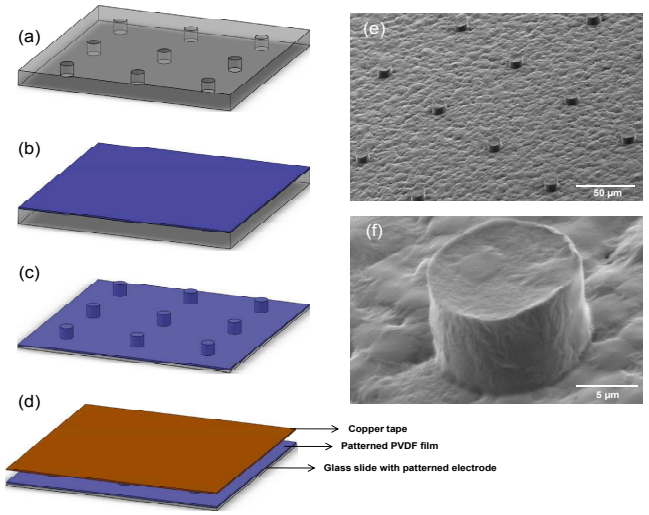

FIGURE 5. PVDF PATTERNING AND SENSOR ASSEMBLY. (A) PATTERNED PDMS MOLD. (B) PVDF SOLUTION IS SPIN COATED OVER THE PDMS. (C) PATTERNED PVDF FILM IS ALIGNED AND TRANSFERRED ONTO THE PATTERNED ELECTRODE. (D) COPPER TAPE IS OVERLAID ON TOP OF THE PILLARS. (E) AND (F) SHOW LOWER AND HIGHER MAGNIFICATION SEM MICROGRAPHS OF THE PVDF PILLARS, RESPECTIVELY.

EXPERIMENTAL VALIDATION AND CHARACTERIZATION

Experimental Setup

The experimental setup shown in Figure 6 was developed and used to conduct various acoustic tests including sensitivity calibration and validation, sensitivity frequency response, and sensor linearity. To calibrate the dynamic response of the sensor, a speaker driven by a sinusoidal wave or band-limited white signal was attached to one end of a circular plane wave tube (PWT). A commercially available microphone, PCB 130C10, was used to benchmark the sensor. The micropillars-based microphone was placed at the opposite end of the PWT next to the commercial microphone. The PWT only propagates the fundamental mode (0,0) plane wave and ensures that the higher order modes are evanescent for various acoustic tests. The output from the micropillar sensor was processed by a custom-made signal conditioning circuit and fed into a data acquisition system (DataPhysics ACE Quattro with SignalCalc softare); the outputs from the commercial microphone were fed directly into the data acquisition system (working in ICP mode).

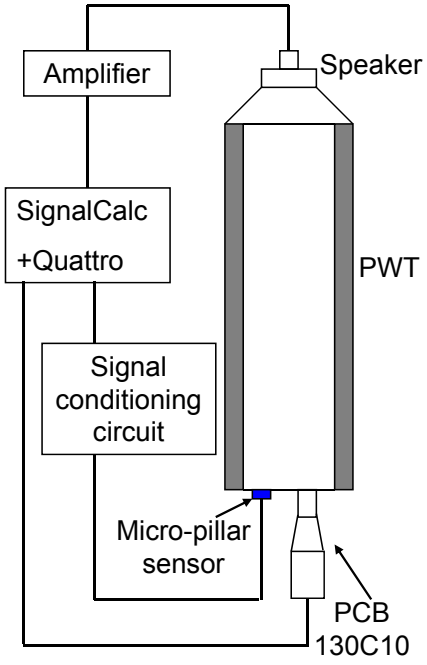

FIGURE 6. SCHEMATIC OF THE EXPERIMENTAL SETUP.

Signal Conditioning Circuit

Figure 7 shows the signal conditioning circuit that was connected to the PVDF sensor. It consists of a buffer circuit with two operational amplifiers in series, two high-pass RC filters and a 60 Hz noise notch filter. The preamplifier circuit is very important for the signal conditioning of the micropillar sensor. A PVDF microphone behaves as a capacitor, hence it generates output voltages with a high impedance level. The source impedance combined with the load resistance provided by the amplifier generates a voltage divider. As the ratio of the load resistance to the source impedance decreases, the output voltage also decreases, which is known as the loading effect. This issue can be addressed by a buffer circuit using an operational amplifier such as the Analog Devices AD712. This amplifier has very high input resistance (300 GΩ), small capacitance (5.5 PF), and small output resistance (around 10 Ω). The buffer circuit converts the

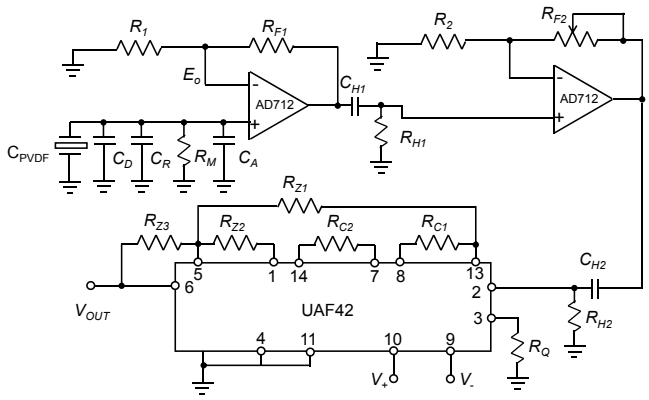

FIGURE 7. SCHEMATIC DIAGRAM OF THE SIGNAL CONDITIONING CIRCUIT.

high output impedance of the microphone into a low impedance signal which eliminates the loading effect and thus minimizes the signal loss. A first-order high-pass filter after the output of each operational amplifier is also utilized to decouple DC voltage and low frequency components generated by thermal effects, which is useful to avoid the potential for signal drift and saturation of the amplifier. Therefore, the first amplifier gain (R_{F1}/R_1) should be relatively smaller compared to that of the second amplifier (R_{F2}/R_2). A total gain of 1000 is used for the acoustic tests. A notch filter can eliminate the 60 Hz noise without seriously degrading the rest of the signal. A notch filter with a notch frequency of 60 Hz and $Q = 10$ was realized with the UAF42 chip and six external resistors. A reduction of approximately 55 dB was measured at 60 Hz.

For many PVDF film based applications, the capacitance of the PVDF film (typically around a few nanofarads) is much larger than the input capacitance of the amplifiers (typically about a few picofarads), which is therefore negligible. However, in terms of the acoustic sensor based on micropillars and patterned electrodes, its capacitance (C_{PVDF}, 9.5 pF) has the same order of magnitude compared to the input capacitance of the operational amplifier (C_A, 5.5 pF) and thus it must be taken into account in the sensitivity calibrations of the sensor. Similarly, the same treatment will be taken for the capacitance (C_R, 3.4 pF) of the parallel resistance, R_M. An additional parallel capacitance, C_D, is critical to the stability of the signal conditioning circuit. If this capacitance is too small, the output of the signal conditioning circuit will be bounded by the dual power supply (± 10 V). A capacitor with capacitance of 104.4 pF was utilized.

Sensitivity Calibration and Validation

The PVDF micropillar sensor and signal conditioning circuit can be modeled as a system comprising a second-order mechanical system, a first-order electrical system, two operational amplifiers in series, two high-pass RC filters, and a 60 Hz noise notch filter. The overall system sensitivity transfer function is

$$K_{mic} = \frac{V_{out}(s)}{P(s)} = \frac{V_{out}(s)}{E_o(s)} \frac{E_o(s)}{P(s)}. \tag{6}$$

The system transfer function between $V_{out}(s)$ and $E_o(s)$ is

$$\frac{V_{out}(s)}{E_o(s)} = \frac{R_{F1}}{R_1} \frac{R_{H1}C_{H1}s}{R_{H1}C_{H1}s+1} \frac{R_{F2}}{R_2} \frac{R_{H2}C_{H2}s}{R_{H2}C_{H2}s+1} H_{nth}(s), \tag{7}$$

in which $H_{nth}(s)$ is the transfer function of the notch filter. The system transfer function between $E_o(s)$ and $P(s)$ has the form [30]

$$\frac{E_o(s)}{P(s)} = \frac{G_1 \tau s}{\tau s+1} \left[G_2 S / \left(\frac{1}{\omega_n^2} s^2 + \frac{2\xi}{\omega_n} s + 1 \right) \right], \tag{8}$$

in which τ is the time constant of the first-order system, ω_n is the natural frequency of the second order system, ξ is damping ratio, S is the footprint of the sensor, and G_1 and G_2 are the gains of the first-order system and second-order system, respectively. Here, $G_1 = K_q/C_t$, where K_q is constant (C/m) and $C_t = C_{PVDF} + C_D + C_R + C_A$ is the total capacitance. $G_2 = 1/k$, where k is the equivalent stiffness of the mechanical system. Therefore,

$$\begin{aligned} \frac{E_o(s)}{P(s)} &= \frac{K_q}{C_t} \frac{\tau s}{\tau s+1} \left[(S/k) / \left(\frac{1}{\omega_n^2} s^2 + \frac{2\xi}{\omega_n} s + 1 \right) \right] \\ &= \left(\frac{C_{PVDF} K_q S}{C_t C_{PVDF} k} \right) \left(\frac{\tau s}{\tau s+1} \right) \left[1 / \left(\frac{1}{\omega_n^2} s^2 + \frac{2\xi}{\omega_n} s + 1 \right) \right], \end{aligned} \tag{9}$$

in which $K_{mpm} = (K_q S)/(C_{PVDF} k)$ is the effective or overall static sensitivity of the sensor, which different from the intrinsic sensitivity given by Eq. (4).

Because the cut-off frequency of the first-order system and high-pass filters is chosen at 20 Hz and the natural frequency of the sensor is much greater than 100 kHz, at 1 kHz the magnitudes of $(R_{H1}C_{H1}s)/(R_{H1}C_{H1}s+1)$, $(R_{H2}C_{H2}s)/(R_{H2}C_{H2}s+1)$, $H_{nth}(s)$, $(\tau s)/(\tau s+1)$, and $\left((1/\omega_n^2)s^2 + (2\xi/\omega_n)s + 1\right)^{-1}$ are nearly 1. Further, $(R_{F1}R_{F2})/(R_1R_2)$ is adjusted to be 1000. Substitution of these values and K_{mpm} into Eqs. (7), (9), and (6) gives

$$K_{mic} = 1000 \frac{C_{PVDF}}{C_t} K_{mpm}, \tag{10}$$

with the overall sensitivity of the sensor as

$$K_{mpm} = K_{mic}\frac{C_t}{C_{PVDF}}\frac{1}{1000} = K_{mic}\frac{C_{PVDF}+C_D+C_R+C_A}{C_{PVDF}}\frac{1}{1000}. \quad (11)$$

It is noted that for most PVDF film based applications the capacitance of PVDF film is typically much greater than the other capacitances such as the input capacitance of the amplifier. In addition, with film there is no need to employ a parallel capacitance to maintain the stability of the signal conditioning circuit. Under this circumstance, the total capacitance is almost equal to the capacitance of the PVDF film and thus the sensitivity of the sensor itself can be simply obtained by only considering the total gain of the signal conditioning circuit. Due to the small capacitance of PVDF micropillars with patterned electrodes comparable to the other capacitances, the measured sensitivity of the sensor should be calculated by Eq. (11) including the capacitance ratio.

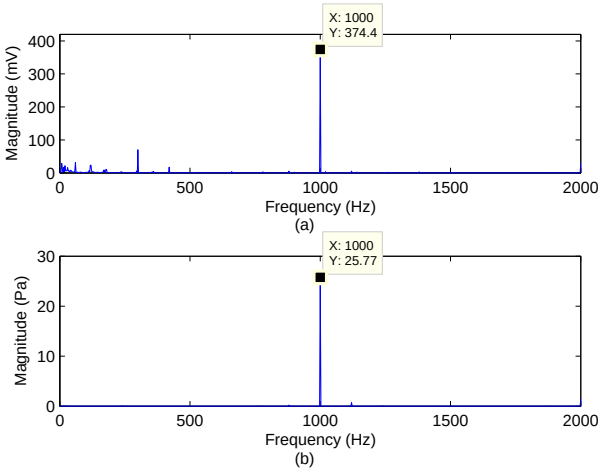

FIGURE 8. COMPARISON OF VOLTAGE SPECTRA OF THE TWO MICROPHONES AT 1 KHZ AND SPL = 124 DB. (A) VOLTAGE SPECTRUM OF THE MICROPILLAR MICROPHONE. (B) VOLTAGE SPECTRUM OF THE REFERENCE MICROPHONE.

The sensitivity calibration tests of the microphone were conducted under 1 kHz sine wave at SPL of ∼120 dB. A PVC pipe with a diameter of 3" and a length of 1 meter was used to generate 1 kHz plane waves. The linear spectrum was obtained by using FFT and a Hanning window. Figure 8 shows the spectra comparison between the two microphones for one test. Figure 9 shows the spectrum waterfall of ten test runs on the two microphones. Table 1 shows the recorded peak values

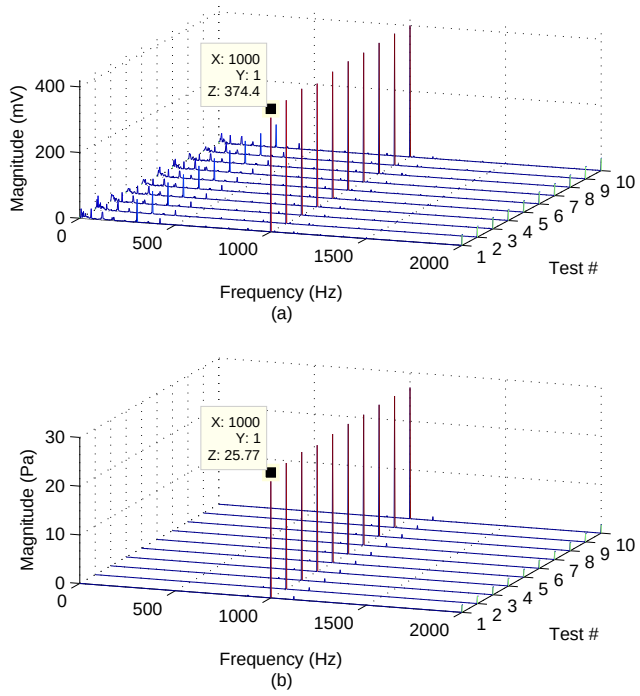

FIGURE 9. SPECTRUM WATERFALL OF THE TWO MICROPHONES AT 1 KHZ AND SPL = ∼120 DB. (A) SPECTRUM WATERFALL OF THE PVDF MICROPHONE. (B) SPECTRUM WATERFALL OF THE REFERENCE MICROPHONE.

at 1 kHz from the double-side spectra of ten test runs. For a sinusoidal wave with an amplitude of A, the double-sided linear spectrum will show a spike with magnitude of A, but the root mean square (RMS) value of the sinusoidal wave is $A/\sqrt{2}$. For the reference microphone having a sensitivity of 19.9 mV/Pa, the mean value of the pressure spikes of ten test runs is 26.49 Pa and thus the RMS pressure is $26.49/\sqrt{2} = 18.73$ Pa, i.e., 119.4 dB. According to this table, the sensitivity of the micropillar microphone (K_{mic}) is 14.647±0.138 mV/Pa, or equivalently −18.343±0.041 dB (re 1 V/Pa). The measured sensitivity of the micropillar sensor (K_{mpm}) is 189.3±1.8 μV/Pa, calculated by $K_{mic}(9.5+104.4+3.4+5.5)/(9.5)(1/1000)$, or equivalently, −37.228±0.041 dB (re 1 V/Pa).

Substitution of K_{mpm} and the thickness of PVDF micropillars, 9.5 μm, into Eq. (3) gives the measured piezoelectric stress constant in the x_3 direction as $g_{33} = -19.93$ V/m/Pa. The stress constant of commercial PVDF film (Measurement Specialties, Inc., USA) is −0.33 V/m/Pa. Therefore, the obtained stress constant amplification ratio is 60.39 (19.93/0.33). The obtained amplification ratio of 60.39 is close to the theoretical prediction of 59.19, thus confirming the performance advantages of the micropillar sensor. The small difference might come from the mask

TABLE 1. PEAK VALUES OBTAINED FROM THE SPECTRUM WATERFALL OF THE MICROPILLAR MICROPHONE AND THE REFERENCE PCB MICROPHONE, AT 1 KHZ

n	1	2	3	4	5	6	7	8	9	10
V_{OUT}(mV)	374.4	375.1	384.6	375.3	386.3	392.6	393.4	398.1	400.6	400.0
P_{PCB} (Pa)	25.77	25.92	26.34	25.96	26.43	26.71	26.79	27.03	26.99	26.95

design, the fabrication errors, the measurements, and the poling process.

CONCLUDING REMARKS

New acoustic sensors with high sensitivity and high frequency bandwidth are needed for addressing emerging requirements of many acoustic, aeroacoustic, and clinical applications. This paper presented the design, fabrication, sensitivity analysis, validation, and characterization of a millimeter-size PVDF acoustic sensor based on a micropillar array and patterned electrodes. Increased sensitivity is achieved through pressure amplification (created by the area ratio between the rigid surface exposed to acoustic waves and the micropillars array) in combination with reduced capacitance (created by a patterned top electrode.)

A PVDF micropillar sensor with patterned electrodes and gap ratio of 5.82 was developed and sensitivity calibration tests were performed on this sensor. The patterned positive photoresist and electrodes were obtained after depositing Au/Pd and selectively removing the photoresist in acetone. Cross sectional analysis confirmed that the patterned micropillars had a height of 9.5 $\pm$0.18 μm. The target dimensions on both the electrodes and pillars were achieved as designed. An experimental setup was developed to characterize the microphone against a reference PCB microphone. A signal conditioning circuit including the preamplifier circuit and the notch filter were developed. The sensitivity calibration test show that the micropillar sensor has a sensitivity of 189.3 μV/Pa, which is 60.39$\times$ greater than that of the commercial PVDF film with the same footprint and thickness. The measured stress constant of the sensor is $g_{33} = -19.93$ V/m/Pa, compared to g_{33} =-0.33 V/m/Pa for commercial PVDF film. The measured stress constant amplification ratio is in good agreement with the predicted amplification ratio of 59.19.

ACKNOWLEDGMENT

We are grateful to the member organizations of the Smart Vehicle Concepts Center (www.SmartVehicleCenter.org) and the National Science Foundation Industry/University Cooperative Research Centers program for supporting this work.

REFERENCES

[1] Arnold, D., and Nishida, T., 2002. "A directional acoustic array using silicon micromachined piezoresistive microphones". *J. Acoust. Soc. Am.,* ***113***, pp. 289–298.

[2] Horowitz, S., Nishida, T., Cattafesta, L., and Sheplak, M., 2007. "Development of a micromachined piezoelectric microphone for aeroacoustics applications". *J. Acoust. Soc. Am.,* ***122***, pp. 3428–3436.

[3] Charleston-Villalobos, S., Cortes-Rubiano, S., Gonzalez-Camarena, R., Chi-Lem, G., and Aljama-Corrales, T., 2004. "Respiratory acoustic thoracic imaging (RATHI): assessing deterministic interpolation techniques". *Med. Biol. Eng. Comput.,* ***42***, pp. 618–626.

[4] Murphy, R., 2004. Patent: Method and apparatus for displaying body sounds and performing diagnosis based on body sound analysis, September.

[5] Kawai, H., 1979. "The piezoelectricity of poly (vinylidene fluoride)". *JPN. J. Appl. Phys.,* ***8***, pp. 975–976.

[6] Tamura, M., Yamaguchi, T., Oyabe, T., and Yoshimi, T., 1975. "Electroacoustic transducers with piezoelectric high polymer films". *Audio Eng. Soc.,* ***23***, pp. 21–26.

[7] Lerch, R., and Sesler, G. M., 1980. "Microphones with rigidly supported piezopolymer membrane". *J. Acoust. Soc. Am.,* ***67***, pp. 1379–1381.

[8] Bloomfield, P., Lo, W., and Lewin, P., 2000. "Experimental study of the acoustical properties of polymers utilized to construct PVDF ultrasonic transducers and the acousto-electric properties of PVDF and P(VDF/TrFE) films". *IEEE T. Ultrason. Ferr.,* ***47***, pp. 1397–1405.

[9] Dias, T., Monaragala, R., and Soleimani, M., 2007. "Acoustic response of a curved active PVDF-paper/fabric speaker for active noise control of automotive interior noise". *Meas. Sci. Technol.,* ***18***, pp. 1521–1532.

[10] Perlman, M., and Canada, M., 1993. Patent: Method to double the piezo-and pyroelectric constant of polyvinylidene fluoride (pvdf) film, October.

[11] Ramos, M., Correia, H., and Lanceros-Mendez, S., 2005. "Atomistic modelling of processes involved in poling of PVDF". *Comp. Mater. Sci.,* ***33***, pp. 230–236.

[12] Dargaville, T., Celina, M., Elliott, J., Chaplya, P., Jones, G., Mowery, D., Assink, R., Clough, R., and Martin, J., 2005. Characterization, performance and optimization of PVDF as a piezoelectric film for advanced space mirror concepts. Tech. Rep. SAND2005-6846, Sandia National

Laboratories.
[13] Lanceros-mendez, S., Silva, V., and Filho, R., 2008. Patent: Non-porous polyvinylidene fluoride (pvdf) films in the beta phase and processing method thereof, August.
[14] Wang, F., Tanaka, M., and Chonan, S., 2003. "Development of a PVDF piezopolymer sensor for unconstrained in-sleep cardiorespiratory monitoring". *J. Intell. Mater. Syst. Struct.*, ***14***, pp. 185–190.
[15] Fujitsuka, N., Sakata, J., Miyachi, Y., Mizuno, K., Ohtsuka, K., Taga, Y., and Tabata, O., 1998. "Monolithic pyroelectric infrared image sensor using PVDF thin film". *Sens. Actuators A,* ***66***, pp. 237–243.
[16] Grosh, K., Zheng, J., deBoer, E., and Nuttall, A. L., 2004. "High frequency electromotility of the cochlea". *J. Acoust. Soc. Am.,* ***115***, pp. 2178–2184.
[17] White, R. D., and Grosh, K., 2005. "Microengineered hydrodynamical cochlear model". *Proc. Natl. Acad. Sci.,* ***102***, pp. 1296–1301.
[18] Arnold, D., Gururaj, S., Bhardwaj, S., Nishida, T., and Sheplak, M., 2001. "A piezoresitive microphone for aeroacoustic measurements". In 2001 ASME International Mechanical Engineering Congress and Exposition, Proc. IMECE '01.
[19] Horowitz, S., Nishida, T., Nishida, T., and Sheplak, M., 2005. "Design and characterization of a micromachined piezoelectric microphone". In 26th AIAA Aeroacoustics Conference, Proc. AIAA.
[20] Z. Wang, C. W., and Liu, L., 2005. "Design and analysis of a PZT-based micromachined acoustic sensor with increased sensitivity". *IEEE T. Ultrason. Ferr.,* ***52***, pp. 1840–1850.
[21] Toda, M., and Thompson, M., 2006. "Contact-type vibration sensor using curved clamped PVDF film". *IEEE Sens. J.,* ***6***, pp. 1170–1177.
[22] Scott, J., Dawber, M., Jiang, A., and Morrison, F., 2003. "New developments in ferroelectric thin films". *Ferroelectrics,* ***286***, pp. 945–957.
[23] Li, J., Rogan, R., Ustundag, E., and Bhattacharya, K., 2005. "Domain switching in polycrystalline ferroelectric ceramics". *Nat. Mater.,* ***4***, pp. 776–781.
[24] Choi, W., Jeon, Y., Jeong, J., Sood, R., and Kim, S., 2006. "Energy harvesting mems device based on thin film piezoelectric cantilevers". *J. Electroceram.,* ***17***, pp. 543–548.
[25] Chu, Y. H., Martin, L., Holcomb, M., Gajek, M., Han, S., He, Q., Balke, N., Yang, C., Lee, D., Hu, W., Zhan, Q., and Yang, P., 2008. "Electric-field control of local ferromagnetism using a magnetoelectric multiferroic". *Nat. Mater.,* ***7***, pp. 478–482.
[26] Hu, Z., Tian, M., Nysten, B., and Jonas, A., 2009. "Regular arrays of highly ordered ferroelectric polymer nanostructures for non-volatile low-voltage memories". *Nat. Mater.,* ***8***, pp. 62–67.
[27] Goel, M., 2003. "Electret sensors, filters and mems devices: New challenges in materials research". *Curr. Sci.,* ***85***, pp. 443–453.
[28] Sohn, J., Choi, S., and Lee, D., 2005. "An investigation on piezoelectric energy harvesting for mems power sources". In Proc IMechE, Vol. 219, pp. 429–436.
[29] Shen, Y., Wejinya, U., Xi, N., and Pomeroy, C., 2007. "Force measurement and mechanical characterization of living drosophila embryos for human medical study". In Proc IMechE, Vol. 221, pp. 99–112.
[30] Xu, J., Dapino, M., Gallego-Perez, D., and Hansford, D., 2009. ""Microphone based on polyvinylidene fluoride (PVDF) micro-pillars and patterned electrodes"". *Sens. Actuators A,* ***153***, pp. 24–32.
[31] Gallego-Perez, D., Ferrell, N., Higuita-Castro, N., and Hansford, D., 2010. "Versatile methods for the fabrication of polyvinylidene fluoride microstructures". *Biomed. Microdevices (in review)*.